Late Quaternary fluvial dynamics and landscape evolution at the lower Shulaveris Ghele River (southern Caucasus)

Hans von Suchodoletz[a]*, Dominik Faust[b]

[a]University of Leipzig, Institute of Geography, Johannisallee 19a, D-04103 Leipzig, Germany
[b]University of Technology Dresden, Institute of Geography, Helmholtzstraße 10, D-01069 Dresden, Germany

Abstract

The southern Caucasus was intensively settled through the Neolithic period to present. Studies of late Quaternary fluvial dynamics and landscape development at the lower Shulaveris Ghele River in southeastern Georgia aid understanding of the Quaternary history of this region. Our studies show that following river aggradation to form a fan-shaped alluvial surface during the late Pleistocene, fluvial sedimentation shifted west, leaving a fan surface subject only to local fluvial and colluvial processes as well as late Neolithic settlement. At about 6 ka, the river avulsed to the east and eroded some late Neolithic settlements occupying the eastern portion of the fan. The avulsion was followed by 3 distinct episodes of aggradation at about 6 ka, 3–2 ka, and since 1.0 ka. No such aggradation is evident in the early Holocene. Regional Holocene fluvial activity in this area was apparently influenced by vegetation dynamics, possibly controlled by regional climatic and/or anthropogenic factors, and significantly differs from the eastern Mediterranean region. All late Neolithic settlements were originally built far from an active river, possibly indicating late Neolithic water management systems.

Keywords: Southern Caucasus; Late Pleistocene; Holocene; Fluvial dynamics; Late Neolithic period; Landscape dynamics; River channel migrations

INTRODUCTION

Landscapes of the southern Caucasus region between the Black and Caspian seas are sensitive to external climatic or anthropogenic controls. This is demonstrated by shrinking or disappearance of mountain glaciers (Gobejishvili, 2004; Messager et al., 2013), varying loess deposition (Wolf et al., 2016), large-scale river migrations (Suchodoletz et al., 2016), and fundamental changes of the vegetation cover (Connor and Kvavadze, 2008; Joannin et al., 2014) during the late Quaternary. However, despite this recent palaeoenvironmental research, knowledge is still limited about former geomorphological processes and environmental conditions in the southern Caucasus. Additional geomorphological and paleoenvironmental research in the southern Caucasus may provide better understanding of: (1) how southern Caucasian landscapes will respond to changing climatic and anthropogenic conditions (Keggenhoff et al., 2014; Gogichaishvili, 2016); and (2) former diachronic human-environmental interactions in this region that was located at the northern periphery of the Near Eastern ancient world and was intensively settled beginning in the Neolithic period (Fig. 1 inset; Lordkipanidze, 2002; Akhundov, 2004; Connor and Sagona, 2007; Fort et al., 2012).

In part to address these questions, we reconstructed late Quaternary fluvial dynamics and landscape development along the lower Shulaveris Ghele River in southeastern Georgia using geomorphologic, stratigraphic, and geochronologic methods. Besides providing information on the regional palaeoenvironmental and geomorphological evolution during the late Quaternary, a second focus of this study is to provide a better palaeoenvironmental context for the late Neolithic Shulaveri settlement group. This settlement group is located in the study area, and its former landscape context is hardly understood so far (Hamon et al., 2016). The group forms part of the well-developed sedentary Shulaveri-Shomutepe (also called Aratashen-Shulaveri-Shomutepe; Chataigner et al., 2014) culture, the first Neolithic culture in semi-humid to arid SE-Georgia, western Azerbaijan, and Armenia that had developed from about 8 ka. Its economy was characterized by a fully developed agro-pastoral economy including the world's first viniculture (Kiguradze, 1986,

*Corresponding author at: University of Leipzig, Institute of Geography, Johannisallee 19a, D – 04103 Leipzig, Germany. E-mail address: hans.von.suchodoletz@uni-leipzig.de (H. von Suchodoletz).
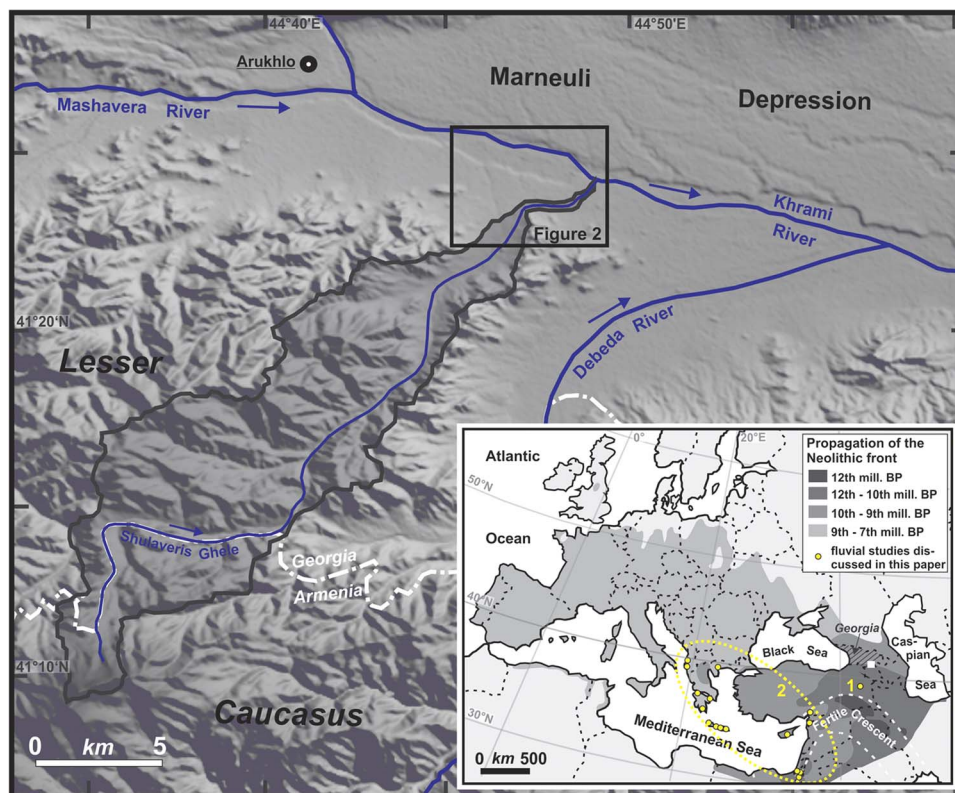
Figure 1. (color online) Map of the study area based on an ASTER-DGM. The catchment of the Shulaveris Ghele River is indicated with a black line. Inset: Location of the study area (white rectangle) at the northern periphery of the Near Eastern ancient world. Propagation of the Neolithic front from the Fertile Crescent towards the North and the West is based on Fort et al. (2012). Georgia is indicated with hatching and the Fertile Crescent with a white dashed line. Other fluvial studies mentioned in this paper: (1) rivers in the Pasinler Basin in eastern Turkey (Collins et al., 2005); (2) compilation of several eastern Mediterranean rivers (Benito et al., 2015). The study of Suchodoletz et al. (2015) is so close that it could not be shown with an own symbol.

2000; Hamon, 2008; Hamon et al., 2016; Lyonnet et al., 2016). Due to its central location in the southern Caucasus, investigations of the Shulaveri settlement group have the potential to significantly contribute to the overall understanding of regional Neolithisation (Hamon et al., 2016).

STUDY AREA

The ~35 km long southwest-northeast directed Shulaveris Ghele (also: Shulavericai) River runs from the Lesser Caucasus Mountains in the Armenian/Georgian borderland into the Marneuli Depression in southeast Georgia (denomination after Maruashvili, 1971) which is the lowest part of the Kvemo Kartli plain. Here, the Shulaveris Ghele flows into the larger Khrami River, which drains via the Kura River into the Caspian Sea. The Shulaveris Ghele catchment covers about 155 km^2 and extends from 2,500 down to 360 m asl. Catchment annual precipitation is as much as 800 mm in the semi-humid Lesser Caucasus Mountains but diminishs to less than 400 mm in the semi-arid Marneuli Depression. The Shulaveris Ghele River is perennial with a mean annual discharge of 0.78 m^3/s and a monthly discharge peak during May of 1.13 m^3/s (data 1976–1985; http://rda.ucar.edu/data/ds553.2/fsu2). The catchment is primarily underlain by

mostly volcanic Cretaceous and Jurassic rocks but also by sandstones, limestones, and marls (Gamkrelidze, 2003). The contemporary natural vegetation of the catchment in the Lesser Caucasus are oak-hornbeam woods and, in the Marneuli Depression, xerophytes and semideserts dominated by Poaceae-Chenopodiaceae-Artemisia associations (Connor et al., 2004; Connor and Kvavadze, 2008).

The Shulaveris Ghele River enters the Marneuli Depression 4 km southwest of its confluence with the Khrami River, forming a fan-shaped alluvial surface inclined about 1.6 % to the northeast towards the Khrami River. The junction of the Shulaveris Ghele with terraces and floodplain of the Khrami River is marked by a several-meter-high scarp. At the apex of the Shulaveris Ghele fan, a relict channel diverges north from the active channel towards the Khrami River (Fig. 2). The current SW-NE eastern river has incised an U-shaped valley into the fan, with a depth between 5 and 7 m and a width of 30 to 40 m. Here, in most parts the Shulaveris Ghele is a meandering single-channel gravel-bed river with some straight segments. Apart from recent incision of about 1 m, no terraces are inset into the valley (Fig. 3A). The inactive western river bed is between 50 and 60 m wide and preserved as an U-shaped valley incised as much as 14 m into the fan-shaped surface. Where it joins the Khrami valley, the
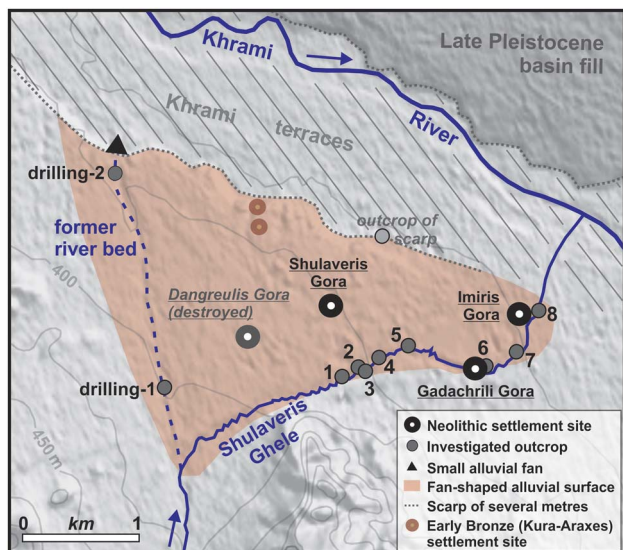
Figure 2. (color online) The study area along the lower course of the Shulaveris Ghele River. DEM-source: ALOS Science Project, Earth Observation Research Center (EORC), Japan Aerospace Exploration Agency (JAXA).

former channel bed ends in a small alluvial fan deposited on a Khrami River terrace with a tread about 9 m above the present river level (Fig. 3B).

The settlements of the late Neolithic Shulaveri settlement group were constructed on the alluvial fan and are preserved as distinct round mounds (tells; Kiguradze, 1986). Erosion by the Shulaveris Ghele subsequent to avulsing to its present eastern course has affected the Imris and Gadachrili Gora settlements (Fig. 3A, inset), whereas the two other settlements Shulaveris and Dangreulis Gora are not eroded by the river. However, Dangreulis Gora was totally destroyed by Soviet excavations (Jalabdadze, M., personal communication, 2016; Fig. 2).

METHODS

Investigations of sedimentary sections

We mapped and sampled the stratigraphy of 9 outcrops along the present eastern course of the lower Shulaveris Ghele River (see exemplary sections in Fig. 4). These sections are exposed along the valley margins and have heights between 4.5 and 7.0 m. Additionally, we conducted two hand drillings of 5 and 2 m depth in the former western river bed using an Eijkelkamp driller (see Fig. 2 for locations and figures in the Supplementary Material for sample positions in the sections).

Sedimentary analyses

Our stratigraphic interpretations relied on identifying fluvial sedimentologic facies and paleosols in conjunction with geochronology. Paleosols indicate former stable geomorphological conditions in a floodplain without significant fluvial sedimentation, and are thus crucial elements of the

fluvial stratigraphy (Faust et al., 2004). To distinguish paleosols from possibly similar-looking sequences in fluvial depositional facies, we in part relied on 33 sample measurements. Our premise was that, for paleosols, carbonate and pH values should systematically decrease (in the up-profile direction), and values of total organic carbon (TOC) and frequency-dependent magnetic susceptibility (χ_{fd}) should increase. In contrast, fluvial depositional facies not altered by in-situ pedogenesis should show less systematic patterns of these properties (Fig. 4; cf. Zielhofer et al., 2009; Suchodoletz et al., 2015).

Carbonate contents were measured following Scheibler in an Eijkelkamp Calcimeter apparatus. Total organic carbon (TOC) was determined by measuring C_{total} with a Vario EL cube elemental analyzer, and subsequently subtracting inorganic carbon taken from carbonate measurements. pH values were measured using a pH-meter 196 (WTW). Frequency-dependent magnetic susceptibility (χ_{fd}) was measured using a Bartington MS3 magnetic susceptibility meter equipped with a MS2B dual frequency sensor (0.465 and 4.65 kHz), and detects mineral grains at the single domain/superparamagnetic border (<30 nm) mostly formed by pedogenesis (e.g., Torrent et al., 2007). For more analytical details the reader is referred to Suchodoletz et al. (2015).

Furthermore, the grain size of 8 representative sediment samples from sections SH-3, SH-7, and SH-8 were measured (see Fig. 5 for locations of the samples). Prior to measurement with a laser-based Malvern Mastersizer S, carbonate was removed with 10 and 30% HCl, organic matter with 10 and 35 % H_2O_2, and the samples were dispersed in sodium pyrophosphate solution ($Na_4P_2O_7$) followed by ultrasonic treatment for 45 minutes.

Numerical dating

The physical stratigraphy and supporting geochemical analyses were bolstered by numerical dating to give a compiled chronostratigraphy along the river. We applied two approaches:

(1) Radiocarbon dating of 12 charcoal pieces embedded into sediment layers and paleosols (see Fig. 5 and the Supplementary Material for GPS coordinates) was performed in the radiocarbon dating laboratories of Mannheim, Germany, Glasgow, UK, and Poznan, Poland. All ages were calibrated using Calpal_A, appying the Intcal13-curve (Reimer et al., 2013). Preferably would have been non-charcoal organic matter (with less possibility of reworking), but such materials were not found.

(2) For luminescence dating, 6 samples were collected from sandy to loamy sediment layers at night (sample positions in the sections see Fig. 5 and the Figures in SOM-1), and processed under subdued red light ($\lambda = 640 \pm 20$ nm) in the Bayreuth luminescence laboratory. After sieving with 200 and 90 μm mesh width, carbonate was destroyed using 10 and 30% HCl and organic matter with 10 and 37% H_2O_2, respectively.
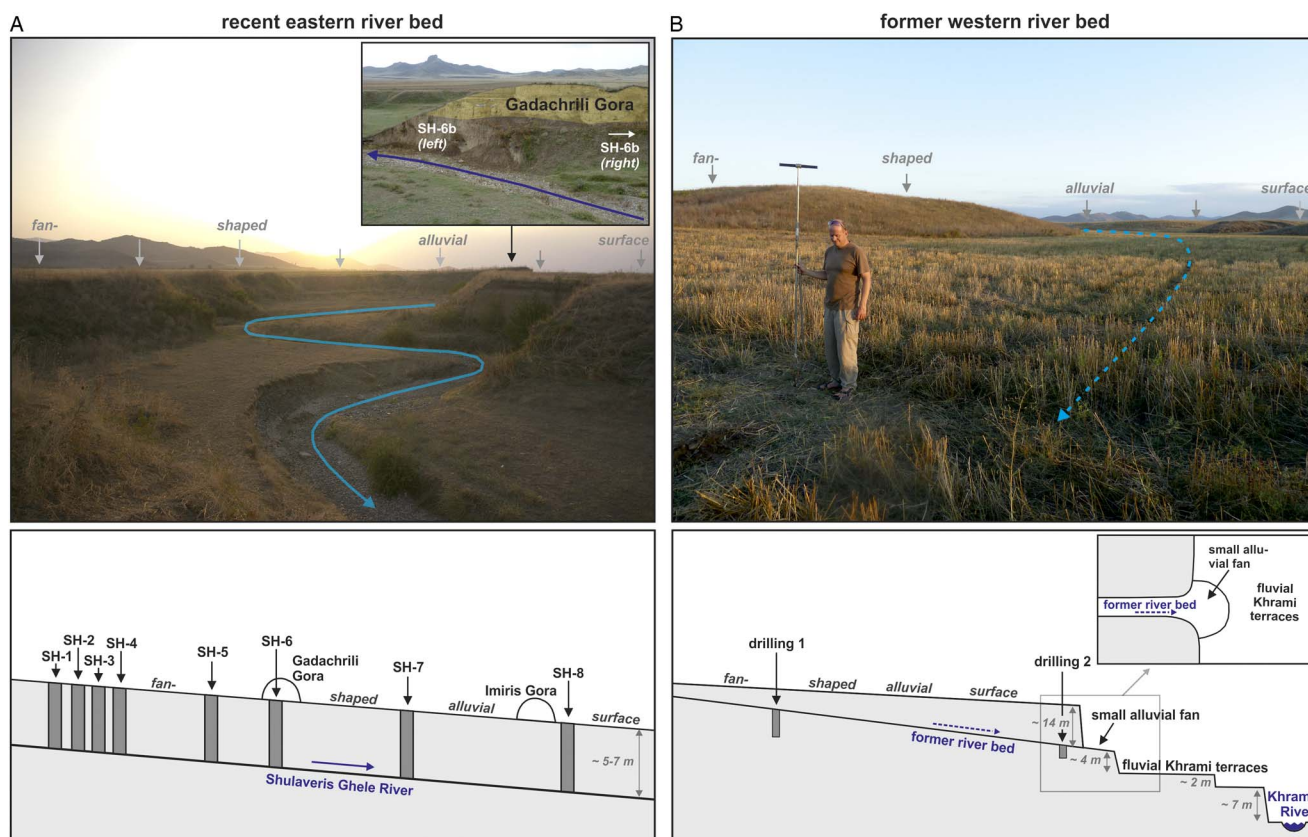
Figure 3. (color online) Views from the north towards the Lesser Causcasus Mountains in the south along the two river beds of the Shulaveris Ghele River (above), and geomorphological sketches with locations of the investigated sections/drillings (below): (A) present eastern river bed, (B) former western river bed. The inset in Figure 3A shows the late Neolithic settlement mound Gadachrili Gora that overtops the surrounding landscape by about 1–2 m and was largely eroded by the Shulaveris Ghele River, as well as the western part of section SH-6b. Due to intensive removal of irrigation water, the lower river course can fall dry during late summer today.

Since the mostly volcanic quartz of the study area is not appropriate for OSL-dating (Gamkrelidze, 2003; Tokuyasu et al., 2010), K-feldspar was separated using sodium metatungstate monohydrate (2.58 and 2.53 g/cm^3). Obtained coarse K-feldspar grains were mounted on aluminium cups (diameter = 12 mm) using silicone oil. Due to generally dim luminescence intensities, sample aliquots of 3 mm were produced. Measurements were performed on a Risø-Reader TL/OSL-DA-15 (Thorn-EMI 9235QA photomultiplier; ^{90}Sr/^{90}Y β-source). We applied the single aliquot regeneration protocol (Murray and Wintle, 2000), including a hotbleach of 280°C after every regenation cycle to reduce recuperation. Stimulation was with infrared LEDs (infrared stimulated luminesence, IRSL), and wavelengths 390–450 nm were detected. No dependence of equivalent doses of preheat temperatures was found during tests. Thus, similar to Preusser (2003), a preheat temperature of 270°C was chosen for equivalent and regenerated doses, and a cut-heat of 200°C for test doses. The first 1.5 s of the signal served to analyse the luminescence signal, and the last 100 s served as background. A recycling ratio larger ± 10% and recuperation >15 % were taken as rejection criteria for individual aliquots. A large scatter of individual De's indicates incomplete bleaching during last sediment transport. Thus, we calculated the De's used for age calculation from the lower part of the De-distribution based on the statistical approach of Juyal et al. (2006) modified by Fuchs et al. (2007), using the simplified minimum age model of Galbraith et al. (1999). To correct for anomalous fading (Huntley and Lamothe, 2001), the g-value of sample L-119 was measured using three aliquots (3.2 ± 1.9). Due to limited machine time and the quite small and geologically homogeneous catchment area, this value was used for all samples.

Dose rates were measured with low-level gamma spectrometry at the Felsenkeller-laboratory of the VKTA Rossendorf in Dresden, Germany, or with thick-source-α–counting (U and Th) and ICPMS (K) at the University of Bayreuth. Since all outcrops had been open for an uncertain period, causing desiccation of the sediments, we inferred a water content of 10 ± 10% for sample L-120 with a sandy grain size. For the orther loamy-textured samples, we inferred a water content of 20 ± 10%. These values should encompass the average water
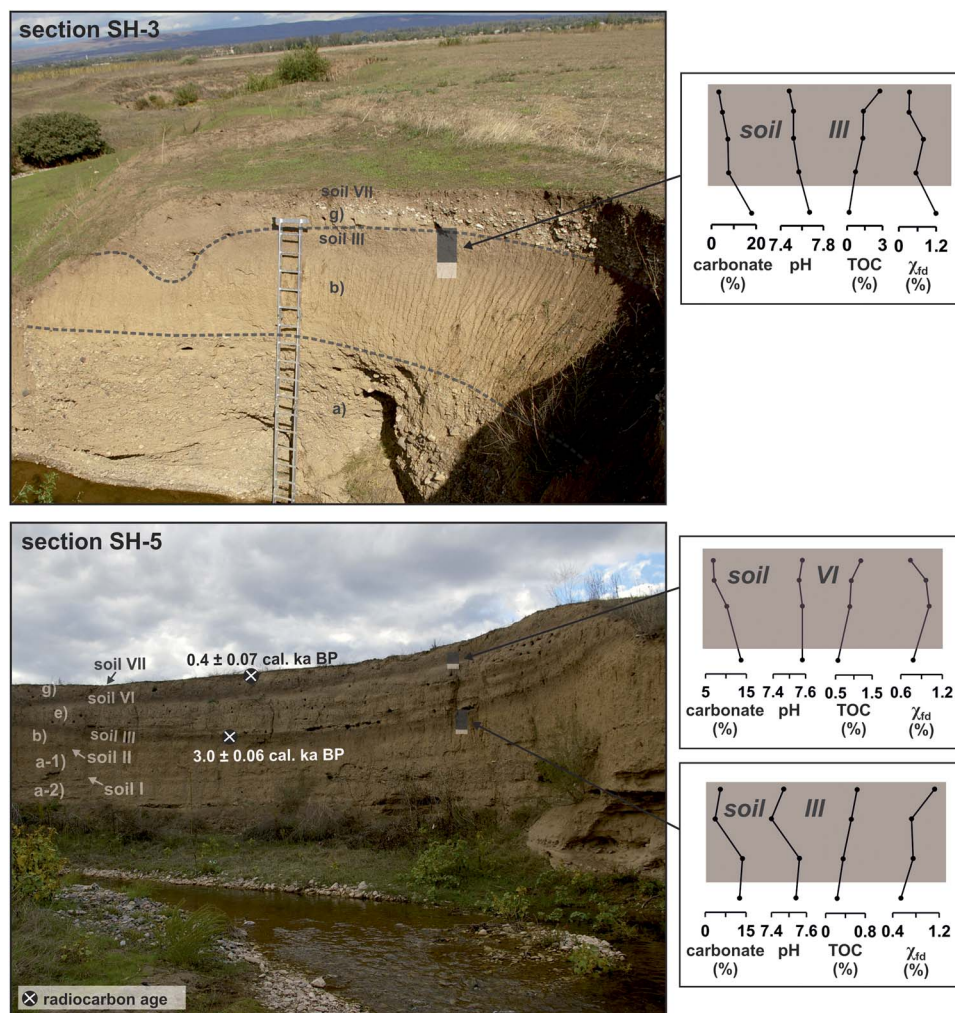
Figure 4. (color online) Two exemplary sections (SH-3 and SH-5) with numerical ages, analytical results, fluvial phases, and paleosols (for the latter see Figures 5 and 6).

content throughout the burial history (Fuchs, 2001). We assumed an internal K-content of 12.5% (Dütsch and Krbetschek, 1997), and an a-value of 0.07 ± 0.02 (Preusser, 2003). Measurement parameters are given in Table 1.

RESULTS

Stratigraphy of the sections

The mapped stratigraphies in conjunction with the analyses supporting paleosol identification (Fig. 4) generally show a consistent sequence that can be correlated between several sections along the present eastern river bed (Fig. 5). Specifically, we identified seven separate episodes of sedimentation (a–g), in part separated stratigraphically by seven paleosols (I–VII). Today, all sediments are deeply incised up to 7 m. The details of the episodes of sedimentation and paleosols are listed in Table 2, and detailed stratigraphies of the sections including interpretations of the sedimentary analyses can be found in the Supporting Online Material (SOM).

    Drilling 1, with a depth of 5 m, was located in the upstream part of the former western river bed, and mostly fluvial sand

fining upwards was found in its lower part. This material is covered by 2-m-thick almost pebble-free loamy sediments that were interpreted as local fluvio-colluvial material. Charcoal was found throughout the drilling. Drilling 2, with a depth of 2 m, was located in the downstream part of the former western river course about 100 m upstream of the small alluvial fan. Basal sandy loam fines upwards and resembles the upper material of drilling 1. Vertic cambisols are found on top of both drillings, underlain by a Ck horizon in drilling 2.

Numerical dating

All radiocarbon samples (Table 3) gave Holocene ages between 7.74 ± 0.06 cal ka BP (sample MAMS-17738) and 0.35 ± 0.07 cal ka BP (sample Poz-40474). Given their positions above younger stratigraphical units, the ages of samples MAMS-17459 (4.8 ± 0.07 cal ka BP, section SH-5) and MAMS-17738 (7.7 ± 0.04 cal ka BP, section SH-6b) must be from incorporation of older charcoal into younger sediments (Table 3; Lang and Hönscheid, 1999). Thus, they are neither shown in Figure 4 and 5. nor further discussed in the text.
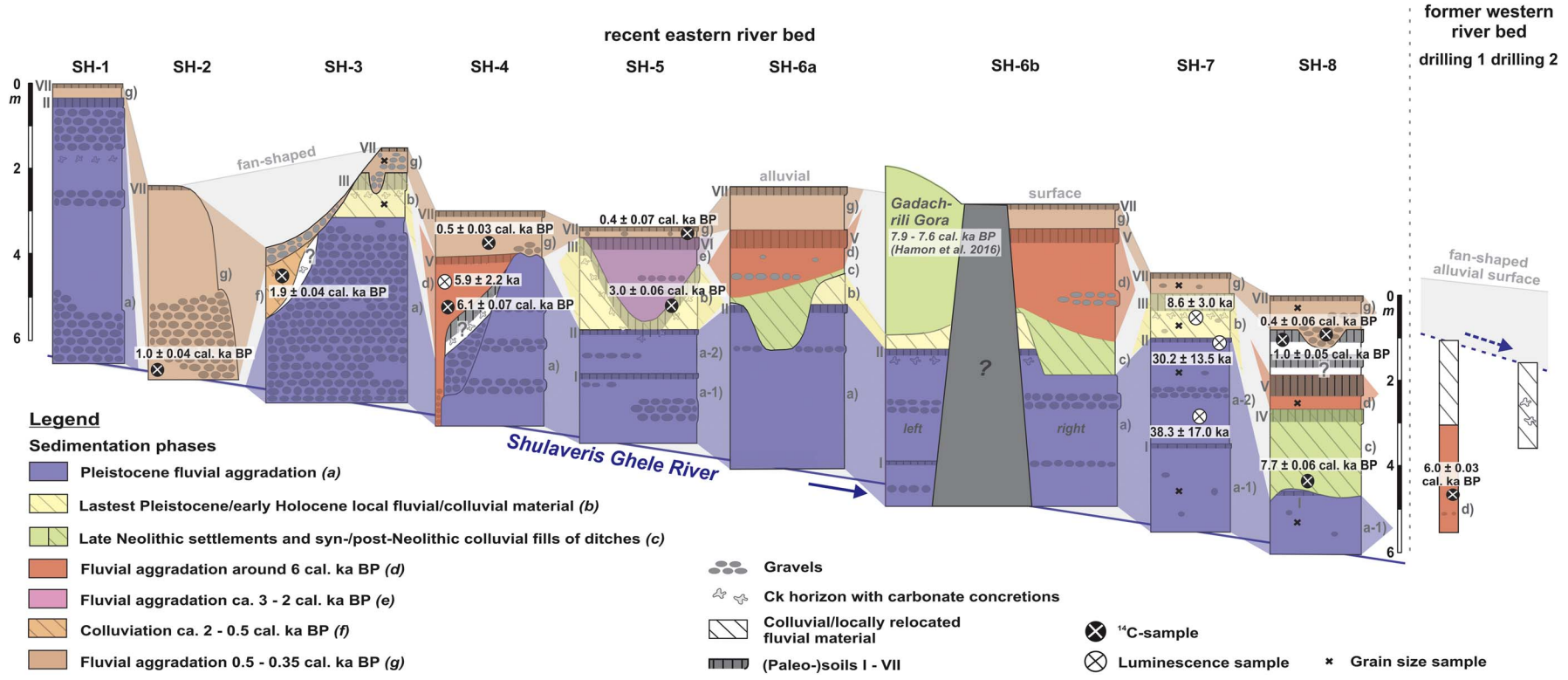
Figure 5. (color online) Schematic compilation of the investigated sections (SH-1–8) along the present eastern river bed, and of the hand drillings (drillings 1 and 2) in the former western river bed. For locations of the sites see Figure 2.

Table 1. Measurement parameters and results of luminescence dating.

Sample number	Section, sample depth (cm)	U-activity (Bq/kg)	Th-activity (Bq/kg)	K-activity (Bq/kg)	Used/total aliquots[1]	De (Gy)	Age (ka)	Corrected age (ka)	Why overestimated?
L-118[2]	SH-4, 180	21.0 ± 3.0	25.9 ± 1.5	426 ± 43	21/36	11.1 ± 1.7	4.3 ± 0.8	5.9 ± 2.2	-
L-119[2]	SH-5, 110	22.0 ± 3.0	26.5 ± 1.5	440 ± 4.4	30/42	11.4 ± 1.1	4.3 ± 0.6	6.0 ± 2.0	Sample is overlying radiocarbon age of 3.0 ± 0.06 cal ka BP.
L-120[3]	SH-6a, 170	12.8 ± 2.2	16.8 ± 2.1	481 ± 14	17/54	21.1 ± 2.0	7.8 ± 1.0	10.9 ± 3.2	Sample is overlying (post-) late Neolithic sediments.
L-150[2]	SH-7, 100	31.0 ± 5.0	32.7 ± 2.1	559 ± 4.6	22/40	18.5 ± 1.3	6.1 ± 0.8	8.6 ± 3.0	-
L-14[2]	SH-7, 170	28.9 ± 2.0	34.4 ± 1.5	630 ± 32	25/26	66.0 ± 3.5	21.1 ± 2.1	30.2 ± 13.5	-
L-110[2]	SH-7, 340	24.0 ± 4.0	30.2 ± 1.9	505 ± 50	29/31	74.2 ± 4.7	26.6 ± 3.3	38.3 ± 17.0	-

[1]Based on the rejection criteria: (i) recycling ratio larger $\pm 10\%$ and (ii) recuperation $>15\%$.
[2]U, Th, and K measured with low-level gamma spectrometry.
[3]U and Th measured with thick-source-α-counting (42 mm), and K measured with ICPMS.

The IRSL-luminescence ages (Table 1) range between late Pleistocene (38.3 ± 17.0 ka, sample L-110) and mid-Holocene (5.9 ± 2.2 ka, sample L-118). All samples showed radioactive equilibrium. Apart from sample L-150 with linear signal growth, the samples showed exponential growth curves. Due to the large error of the applied g-value, the ages show rather large error bars after fading correction. Furthermore, the applied fading correction after Huntley and Lamothe (2001) generally only works for samples with linear growth. However, because IRSL is the only luminescence dating technique appropriate in this volcanic environment, these are the ages we have to work with, but they should be regarded as approximate. Given their positions above younger stratigraphical units, the ages of samples L-119 (6.0 ± 2.0 ka, section SH-5) and L-120 (10.9 ± 3.2 ka, section SH-6a) must be too old, possibly because of insufficient bleaching that often occurs in fluvial environments (Table 1; Rittenour, 2008). Thus, they are neither shown in Figures 4 and 5 nor further discussed in the text.

DISCUSSION

Late Quaternary fluvial dynamics and landscape evolution at the lower Shulaveris Ghele River

By combining the compiled stratigraphy and numerical dating, late Quaternary fluvial dynamics and landscape evolution along the lower Shulaveris Ghele River could be reconstructed as follows (Fig. 5 and 6).

Late Pleistocene (Fig. 6A)

Fluvial sediments fining downstream were aggraded along the present eastern course (sedimentation phase a). Similar sediments were also observed in the central part of the former alluvial surface in an outcrop at the scarp with the Khrami valley (see Fig. 2 for location). Thus, the surface was apparently formed by fan-like fluvial aggradation. After leaving the confined valley in the Lesser Caucasus, the river aggraded large quantities of sediments as sheets or stream channel

fillings on a radial surface. The fining downstream indicates less stream channel fillings but more sheetflood deposits due to less fluvial energy in that peripheral region (Bull, 1972). Consequently, the larger preservation potential allowed preservation of intercalated soil I only in that part of the surface. This soil indicates geomorphic stability due to incision, less frequent flooding, and/or shifting aggradation. Sediments of sub-phase (a-2), deposited above soil I, were IRSL-dated between 38.3 ± 17.0 ka (L-110) and 30.2 ± 13.5 ka (L-14). Following this, soil II was formed, that is, exposed in the downstream part of the surface. The apparent absence of river sediments along the present eastern river course between about 30 ka and mid-Holocene may indicate river incision and/or a shift of fluvial sedimentation onto a more western part of the alluvial surface, allowing formation of soil II.

Latest Pleistocene/early Holocene (Fig. 6B)

Along the present eastern river course, soil II is covered by mostly gravel-free loam (sedimentation phase b). Given missing gravel layers and band and a very similar grain size with sediments of preceding phase (a) (Fig. 7), these sediments were probably derived from the latter and deposited by local fluvio-colluvial processes. A Ck horizon below soil II in section SH-6b indicates a longer stable period without sedimentation but soil formation following phase (a). Thus, phase (b) must have started some millenia after about 30 ka. In section SH-7 its sediments were IRSL-dated to 8.6 ± 3.0 ka (L-150). However, a well-developed Ck horizon demonstrates intensive development of soil III that had formed on top of these sediments. Thus, soil III must have formed during several millenia so that the IRSL-age probably dates the very end of phase (b). Linked with regional fluvial incision around the Pleistocene/Holocene transition (Suchodoletz et al., 2015, 2016; Ollivier et al., 2015, 2016), the Khrami River was also incised, forming the scarp between the alluvial surface and the Khrami valley. This must have led to incision of the former western river course, causing final abandonment of the fan-shaped alluvial surface. The

Table 2. Detailed information on late Quaternary sedimentation phases and (paleo-) soils found along the present eastern river bed of the lower Shulaveris Ghele River.

Sedimentation phases (a–g)/soil formation periods (I–VII)	Sediment/soil properties; indicators for incision	(Max.) thickness	Significant charcoal, prehistoric artifacts	Exposed in sections
a-1 *(fluvial)*	Loamy to gravelly	2 m	-	SH-5, 6b, 7, 8 (downstream)*
soil I *(luvisol)*	Reddish Bt-horizon with slight clay coatings	10 cm	-	SH-5, 6b, 7, 8 (downstream)*
a-2 *(fluvial)*	Loamy to gravelly	2.5 m	-	SH-5, 6b, 7, 8 (downstream)*
soil II *(luvisol)*	Reddish Bt-horizon with intensive clay coatings; in section SH-6b, underlain by Ck horizon with small carbonate concretions	10 cm	-	SH-1, 5, 6a, 6b, 7
b *(colluvial)*	Brownish to yellowish loam with singular pebbles	2 m	-	SH-3, 5, 6a, 6b, 7
soil III *(cambisol)*	• Brownish Bw-horizon underlain by Ck-horizon with large carbonate concretions • In section SH-5, preceded by incision	40–50 cm	-	SH-3, 5, 7
c *(colluvial)*	Sandy to loamy archaeosediments with singular pebbles and organic layers derived from late Neolithic settlements that were built on/into sediments of phases (a) and (b)	2.5 m	charcoal, bones, ash, potsherds, obsidian artifacts	SH-6a, 6b, 8
soil IV *(fluvisol)*	Very weakly developed Ah-horizon	20 cm	-	SH-8
d *(fluvial)*	• Gravelly • Valley almost filled up to recent surface; in section SH-4 discordantly covering paleosol of unknown age and type extending down to 1.5 m above recent river bed → preserved valley form along present eastern river bed and incision prior to phase (d)	4 m	singular charcoal, potsherds, bones	SH-4, 6a, 6b, 8
soil V *(cambisol)*	Brownish Bw-horizon	30 cm	-	SH-4, 6a, 6b, 8
e *(fluvial)*	• Loamy to gravelly • Base about 1 m lower than upper limit of sediments from previous phase (d) → some incision prior to phase (e)?	1.8 m	charcoal	SH-5
soil VI *(cambisol)*	Greyish-brownish Bw-horizon	40 cm	-	SH-5
f *(colluvial)*	• Gravel-free loam with relocated carbonate concretions • Extending down to 3.5 m above recent river bed = much lower than sediments of preceding phase (e) → incision prior to phase (f)	1.2 m	charcoal, potsherds	SH-3
g *(fluvial)*	• Gravelly • Valley filled from present river bed up to recent surface	4.5 m	charcoal	SH-1, 2, 3, 4, 5, 6a, 6b, 7, 8
soil VII *(fluvisol)*	Weakly developed Ah-horizon	5–10 cm	-	SH-1, 2, 3, 4, 5, 6a, 6b, 7, 8

*In the upstream sections (SH-1, SH-3, and SH-4), the sediments of phase (a) are much more gravelly than downstream and are not divided by soil I.

observed incision of sediments of phase (b) prior to formation of soil III was possibly also linked with that process.

Late Neolithic period (Fig. 6C)

During the eighth millenium BP, the settlements Imiris and Gadachrili Gora were constructed at the edge of the present eastern river course, where an inactive valley form must have been preserved. Reported radiocarbon ages for Gadachrili Gora vary between 7.9 and 7.6 cal ka BP (Hamon et al., 2016;

Kvavadze et al., 2010), and a radiocarbon age of Imiris Gora gave 7.2 ± 0.15 cal ka BP (Kiguradze, 1986).

Late Neolithic/post-late Neolithic period (Fig. 6D)

The Neolithic ditches were filled up with loamy archaeosediments (sedimentation phase c). Charcoal from these sediments was radiocarbon dated to 7.7 ± 0.06 cal ka BP (Poz-40477), falling into the settlement period of Gadachrili Gora. However, colluvial filling of the ditches probably

Table 3. Results of radiocarbon dating of charcoal pieces.

Sample number*	Section, sample depth (cm)	Embedded in	$\delta^{13}C$ (%)	^{14}C age (ka BP)	Calibrated ^{14}C-age (cal ka BP)	Why overestimated?
Poz-40472	SH-2, 410	Fluvial sediment layer	−22.2	1.10 ± 0.03	1.01 ± 0.04	-
SUERC-38291 (GU26188)	SH-3, 350	Colluvial deposit	−24.4	1.91 ± 0.03	1.87 ± 0.04	-
SUERC-38292 (GU26190)	SH-4, 150	Fluvial sediment layer	−25.9	0.42 ± 0.03	0.48 ± 0.03	-
MAMS-17460	SH-4, 230	Fluvial sediment layer	−29.1	5.35 ± 0.02	6.11 ± 0.07	-
Poz-40474	SH-5, 30	Fluvial sediment layer	−24.2	0.27 ± 0.03	0.35 ± 0.07	-
MAMS-17459	SH-5, 150	Fluvial sediment layer	−27.3	4.21 ± 0.02	4.76 ± 0.07	Sample is overlying radiocarbon age of 3.0 ± 0.06 cal ka BP
Poz-40473	SH-5, 210	Paleosol	−24.4	2.90 ± 0.04	3.03 ± 0.06	-
MAMS-17738	SH-6b, 150	Fluvial sediment layer	−25.2	6.90 ± 0.03	7.73 ± 0.04	Sample is overlying (post-) late Neolithic sediments
Poz-40480	SH-8, 60	Fluvial sediment layer	−29.7	0.28 ± 0.04	0.37 ± 0.06	-
Poz-40478	SH-8, 120	Paleosol	−34.4	1.09 ± 0.04	1.01 ± 0.05	-
Poz-40477	SH-8, 480	Fluvial sediment layer	−29.8	6.90 ± 0.06	7.74 ± 0.06	-
MAMS-17458	SH-drilling 1, 410	Fluvial sediment layer	−25.4	5.23 ± 0.02	5.97 ± 0.03	-

*POZ, Poznan Radiocarbon Laboratory; MAMS, Mannheim Radiocarbon Laboratory; SUERC, Scottish Universities Environmental Research Centre, Glasgow.

started/resumed after the late Neolithic period, so this age possibly slightly overestimates sediment deposition. The sediments of phase (c) were overprinted by weakly developed soil IV.

Around 6 cal ka BP (Fig. 6E)

Charcoal from coarse sandy river sediments from drilling 1 in the western former river bed were radiocarbon-dated to 6.0 ± 0.03 cal ka BP (MAMS-17458). Overlying local fluvio-colluvial sediments were also found in drilling 2 about 2 km downstream (Fig. 2). Thus, the radiocarbon age apparently dates the last river activity in that river bed, where subsequently only local fluvio-colluvial processes occurred. A longer inactive period of the western river bed is also supported by a well-developed Ck horizon below the recent soil in drilling 2, demonstrating long-lasting soil formation until today. The low-energy local fluvio-colluvial processes could not incise the Khrami terrace down to the recent Khrami channel, i.e., the recent erosion base. Instead, the small alluvial fan at the outlet of the former western river bed was aggraded (Fig. 3B).

For the now-active present eastern river course, a radiocarbon age of 6.1 ± 0.07 cal ka BP (MAMS-17460) and an IRSL age of 5.9 ± 2.2 ka (L-118) were obtained from gravelly-to-loamy river channel sediments in section SH-4. Thus, following a long inactive period, fluvial aggradation (sedimentation phase d) apparently restarted along that river bed during that time. The measured grain size of sediments deposited since then is much coarser than that of phases (a) and (b) (Fig. 7), and numerous gravel layers and bands are observed. Similar gravelly to loamy channel sediments cover

the post-Neolithic archaeosediments of phase (c) in sections SH-6a, SH-6b, and SH-8. Because there is only slight evidence of soil formation between these sediments and those of phase (c) (soil IV; Fig. 5), the former must have been deposited quite shortly after the late Neolithic period. Thus, they were also classified into sedimentation phase (d).

Between about 6 and 3 cal ka BP (Fig. 6F)

Formation of soil V and perhaps some incision of the present eastern river bed occurred, and no fluvial sediments originate from this period.

Between about 3 and 2 cal ka BP (Fig. 6G)

Gravelly to loamy channel sediments were aggraded along the present eastern river bed (sedimentation phase e). The timing of aggradation is indicated by (1) the radiocarbon age of 3.0 ± 0.06 cal ka BP of charcoal from the upper part of underlying soil III in section SH-5 (Poz-40473); (2) a radiocarbon age of 1.9 ± 0.04 cal ka BP from colluvial sediments of following phase (f); and (3) the well-developed paleosol VI in section SH-5 that separates the sediments of phases (e) and (g), demonstrating a significant time gap between both phases (Fig. 5).

About 2 – 0.5 cal ka BP (Fig. 6H):

Strong incision of the present eastern river bed must have occurred at the beginning of this period, probably allowing formation of soil VI. According to the radiocarbon age of 1.9 ± 0.04 cal ka BP (SUERC-38291) of charcoal from a
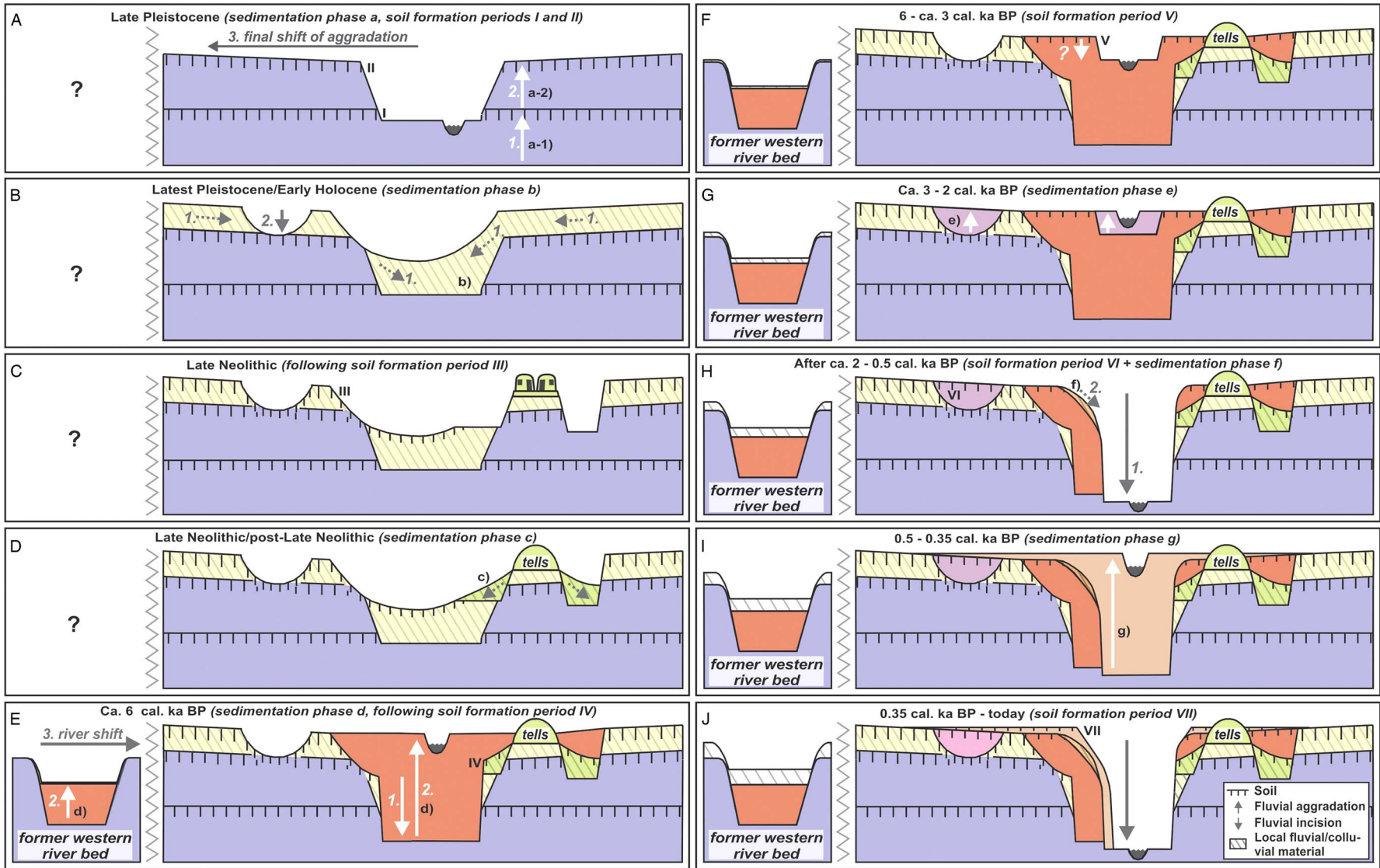
Figure 6. (color online) Late Quaternary landscape development along the lower Shulaveris Ghele River. Colours and symbols used for the sediments of the different phases are taken from Figure 5.
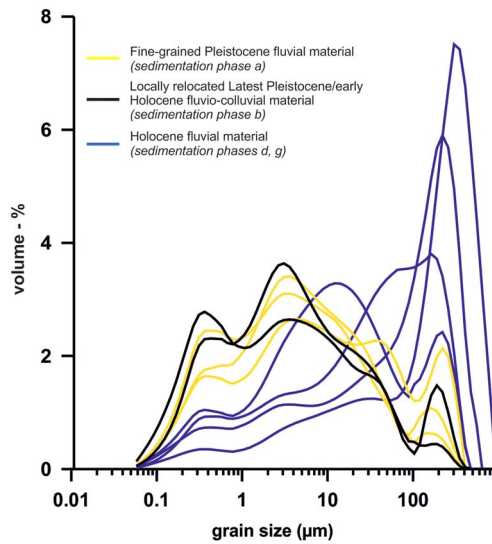
Figure 7. (color online) Results of selected grain size analyses from sections SH-3, SH-7, and SH-8. The locations of the samples in the stratigraphies can be seen in Figure 5.

colluvial deposit in section SH-3, this also allowed colluviation along the present eastern river bed (sedimentation period f). No fluvial sediments originate from this period.

About 0.5 – 0.35 cal ka BP (Fig. 6I)

Intensive gravelly to sandy fluvial aggradation along the present eastern river bed spilled over on the adjacent surface (sedimentation phase g). Radiocarbon ages of these sediments are 0.48 ± 0.03 cal ka BP (SUERC-38292, section SH-4), 0.37 ± 0.06 cal ka BP (Poz-40480, section SH-8), and 0.35 ± 0.07 cal ka BP (Poz-40474, section SH-5). Their base was radiocarbon dated to 1.0 ± 0.04 cal ka BP (Poz-40472, section SH-2) and charcoal from the soil underlying these sediments in section SH-8 gave an age of 1.0 ± 0.05 cal ka BP (Poz-40478). This demonstrates still strong incision of the river about 1 cal ka BP and a later start of significant aggradation.

After about 0.35 cal ka BP – today (Fig. 6J)

During this time the present eastern river bed was incised by up to 7 m, allowing formation of soil VII.

Possible controls of the late Quaternary dynamics of the Shulaveris Ghele River

In the following, we compare our fluvial record with a similar study carried out ca. 10 km to the northeast along the lower
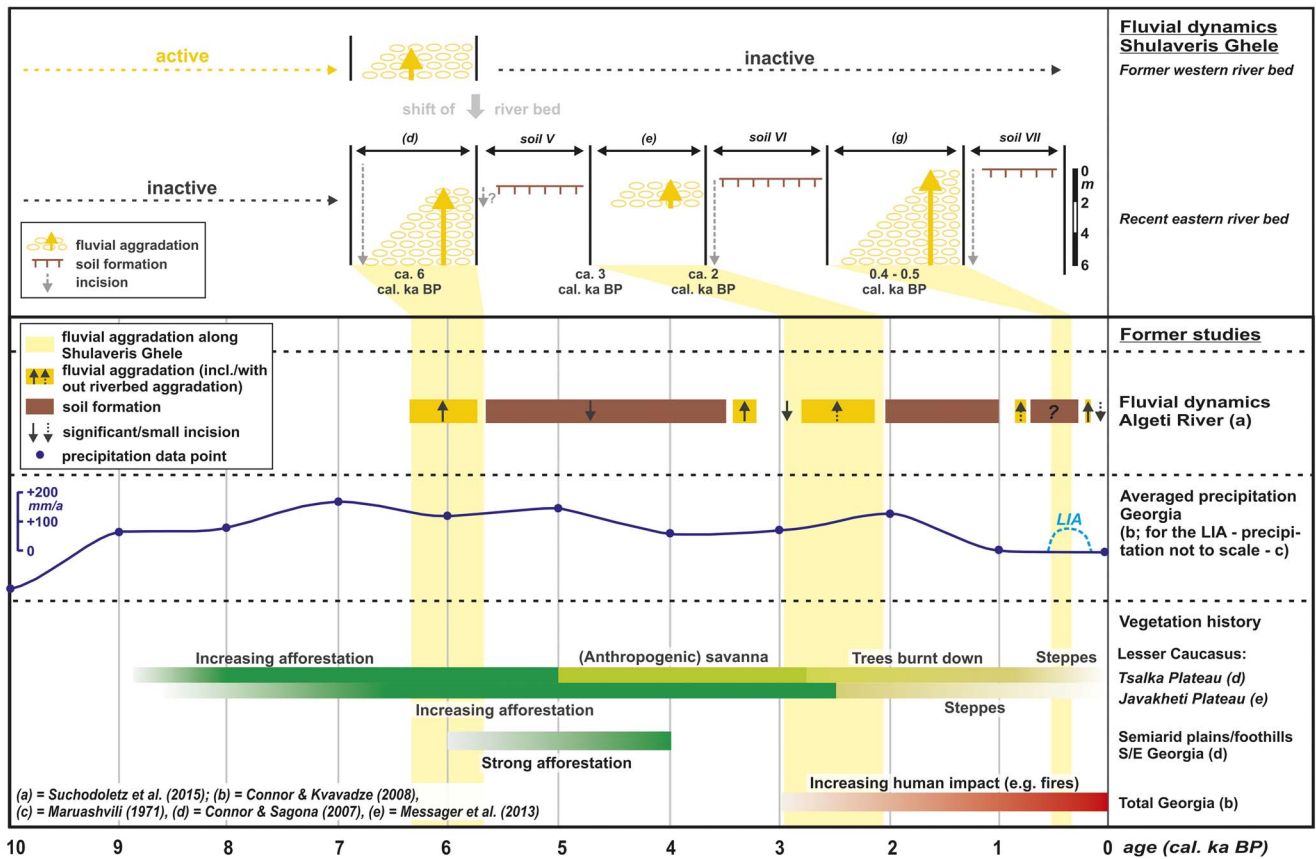

Figure 8. (color online) Comparison of the Holocene fluvial dynamics of the lower Shulaveris Ghele River with other regional paleoenvironmental records. Shadowed areas indicate periods of fluvial aggradation along the lower Shulaveris Ghele River, and according to information given by Maruashvili (1971) the Little Ice Age (LIA) was also shown as a humid period whereof the duration was taken from Mann (2002).

Algeti River (Suchodoletz et al., 2015), as well as with other regional paleoenvironmental and historical studies (Fig. 8).

Besides gravels, the late Pleistocene fan-shaped alluvial surface is largely formed by sand and silt (Fig. 7). The later sub-phase (a-2) was dated between about 40 and 30 ka. Intensive aggradation of fine sandy and silty sediments is also known from other regional rivers between about 42 and 20 ka (Suchodoletz et al., 2016). Similar to neighbouring regions of Eurasia and Iran (Dodonov et al., 2006; Vlaminck et al., 2016), late Pleistocene loess sedimentation is also described for northern Armenia (Wolf et al., 2016). Thus, the large proportion of silt in regional fluvial sediments of late Pleistocene age can possibly also be explained with aeolian input.

The possible shift of fluvial activity towards the western part of the alluvial surface was followed by a stable period with soil formation along the present eastern river bed. Subsequently, during latest Pleistocene/early Holocene loamy sediments of phase (a) were relocated by local fluvio-colluvial processes (sedimentation phase b). Regional pollen studies indicate a significant precipitation increase between 10 and 8 ka (Connor and Kvavadze, 2008; Joannin et al., 2014). Thus, before that period, the semiarid to arid landscape was only sparsely vegetated and largely instable, which allowed sediment mobilisation and redeposition. However, it cannot be resolved whether these processes correlated with short-term climatic events such as around 10.3 and 8.2 ka as supposed for slope deposits in Europe or Anatolia (Dreibrodt et al., 2010; Vincent et al., 2010; Dreibrodt et al., 2014).

Following deep incision of the regional rivers around the Pleistocene/Holocene transition (Suchodoletz et al., 2015, 2016; Ollivier et al., 2015, 2016), no aggradation was recorded along the neighbouring Algeti River until about 6 ka, whereas no data are available for the Shulaveris Ghele (Fig. 8). Either there was no significant fluvial aggradation, or aggraded sediments were swept out during following periods. As noted earlier, precipitation significantly increased between 10 and 8 ka (Connor and Kvavadze, 2008; Joannin et al., 2014), and the higher parts of the Lesser Caucasus were intensively afforested (Connor and Sagona, 2007; Messager et al., 2013). Although the lowlands and plains were still covered by dry savannas, dense gallery and riparian forests were found along the rivers (Connor and Sagona, 2007; Chataigner et al., 2014; Lyonnet et al., 2016). This indicates a largely stabilized landscape resulting in relatively weak fluvial dynamics without significant aggradation. Accordingly, Shulaveri-Shomutepe settlements in western Azerbaijan were built on pre-Neolithic alluvial fans that were covered by new sediments only since about 5.2 ka (Ollivier et al., 2016).

Both the Algeti and Shulaveris Ghele rivers aggraded around 6 ka, when the climate was relatively cool (Connor and Sagona, 2007) and dry (Fig. 8; Connor and Kvavadze, 2008). Furthermore, their semiarid lower catchments were still not forested (Fig. 8; Connor and Sagona, 2007) so that sediment mobilization was still easily possible here. Thus, a climatic deterioration affecting a partly fragile landscape could possibly have caused middle Holocene aggradation (Suchodoletz et al., 2015).

Between about 3 and 2 ka, Algeti and the Shulaveris Ghele River aggraded again. Human impact on the regional vegetation significantly increased during that period (Connor and Kvavadze, 2008), and especially the upper catchments in the Lesser Caucasus were largely deforested (Connor and Sagona, 2007; Messager et al., 2013). This could have mobilized large quantities of sediment, causing the observed aggradation.

During the last 1 ka, both rivers showed similarities and differences. Sedimentation along the Algeti River between 0.77 and 0.72 ka was possibly caused by intensive deforestation during a high cultural phase of the Georgian state (Lordkipanidze, 2002). The Little Ice Age (LIA) between the fifteenth century and AD 1850 (Mann, 2002) was reported as a more humid period in the southern Caucasus (Maruashvili, 1971), which could be a possible cause of fluvial aggradation. Aggradation occurred along the Shulaveris Ghele between 0.5 and 0.35 ka, and along the Algeti between 0.2 and 0.15 ka. Although the latter period could also be caused by a Persian invasion with large-scale destruction of cities and agricultural land (Lordkipanidze, 2002), its timing at the end of the LIA could also indicate a climatic cause. Likewise, rivers in the European Alps and the northwest Mediterranean basin showed increased activity linked with more humid conditions at least during parts of the LIA (Wirth et al., 2013; Benito et al., 2015).

Altogether, similar fluvial patterns of both rivers were probably caused by regional paleoenvironmental signals, and existing differences could possibly be explained with different tectonic settings, small-scale variations of natural or anthropogenic conditions, or different internal thresholds of the rivers (Leopold et al., 1964). Comparing our fluvial aggradation periods of ~6 ka, 3–2 ka, and since about 1 ka with neighbouring regions, they are very different from the eastern Mediterranean basin where flooding occurred 8–7 ka, around 4 ka, and since about 2 cal ka BP (Fig. 1 inset; Benito et al., 2015). For the Pasinler Basin in eastern Anatolia, overbank sedimentation was described between 8.6 and 5.7 ka, and fluvial aggradation resumed since about 1 ka (Fig. 1, inset; Collins et al., 2005). Due to dating uncertainties, the first sedimentaton period could not be correlated with aggradation in our study area, but the second period resembles our last aggradation period. Thus, the fluvial dynamics in the southern Caucasus apparently shows some similariaties with eastern Anatolia but strongly differ from those of the eastern Mediterranean basin. Whereas both eastern Anatolia and southern Caucasus show a main precipitation peak during May, the eastern Mediterranean basin is characterized by maximal winter precipitation and discharge, which could explain the very different fluvial patterns.

Late Neolithic settlement activity and evolution of the surrounding landscape

Our study suggests that the lower Shulaveris Ghele River did not flow in its present eastern bed during the time of the Shulaveri-Shomutepe culture, and only came back about

6 cal ka BP. This finding is based on: (1) missing fluvial sediments along the present eastern river course between about 30 ka and 6 ka; (2) a well-developed former western river bed that is incised into the fan-shaped alluvial surface and ends at a 9-m-high terrace of the Khrami River. This river bed must have been active during the Pleistocene/Holocene transition when the alluvial surface was incised, and fluvial activity must have persisted until about 6 ka, when the 9 m Khrami terrace was formed (Hans von Suchodoletz, unpublished data); (3) fluvial sediments in the former western river bed that apparently represent the last fluvial activity and are concomitant with the restart of fluvial activity in the present eastern river bed about 6 ka.

Thus, although located next to the present eastern river bed, the late Neolithic settlements Imiris and Gadachrili Gora did not have direct access to the river. Accordingly, their location could not be explained with the search for direct water access as was supposed by Hamon et al. (2016). Instead, similar to Dangreulis and Shulaveris Gora, the settlements were constructed some kilometers away from any river. Likewise, the late Neolithic settlement Arukhlo (north of the Mashavera River; Fig. 2) also was constructed at an elevated position in a distance of about 1 km from the neighbouring rivers. The lack of direct water access and of (yet discovered) wells suggests that water supply of Imiris and Gadachrili Gora could have been facilitated by water management systems similar to those described for other Neolithic cultures in semi-humid to arid regions of the Near East (Gillmore et al., 2009; Mithen, 2010). These could have been freshwater canals, as was hypothesized for a canal that was excavated next to Imiris Gora (Javakhishvili, 1973), or ditches that served as water reservoirs, as was formerly assumed for Arukhlo (Kiguradze, 1986; Hansen et al., 2007). The valley form at the place of the present eastern river bed, apparently preserved between the late Pleistocene and middle Holocene, could have facilitated the construction of canals. Interestingly, in contrast to Shulaveris Gora that was located far from any preserved valley (Fig. 2), no water reservoirs are described for Imiris and Gadachrili Gora (Javakhishvili, 1973; Hamon et al., 2016). Looking further into the archaeological record of Gadachrili Gora, the absence of river activity in the present eastern river bed prior to about 6 ka excludes varying river activity as a cause of the diachronically varying late Neolithic settlement organization as was supposed by Hamon et al. (2016).

In the following, we will discuss potential causes for the Holocene river channel migration that is a key feature to understanding the late Neolithic landscape context of the study area.

Tectonically-induced lateral ground tilting can cause river channel migrations (Holbrook and Schumm, 1999; Sahu et al., 2010). However, significant faults are only found about 15 km to the south in the Lesser Causasus (Gamkrelidze, 2003) and, unlike some parts of the Lesser and Greater Caucasus, no earthquakes were recorded significantly north of these faults, at least during the twentieth century (Berberyan, 1997; Suchodoletz et al., 2016). Although only covering a relatively short period, these data and missing large faults indicate that the study area must have been tectonically relatively quiet, at least at the Holocene time scale. Furthermore, the suggested switching of fluvial aggradation from east to west and back again argues against a continuous tilting trend, making a tectonic cause for the river channel migration unlikely.

The channel migration around 6 ka falls into the transition between the Chalcolithic Sioni and the early Bronze Kura Araxes cultures in eastern Georgia (Kiguradze, 2000; Connor and Sagona, 2007). Sioni settlement is documented about 15–20 km to the south (Nebieridze, 2010), and Kura Araxes settlements are found in the study area at the scarp between alluvial surface and Khrami valley (Fig. 2; Jalabadze, M., personal communication, 2016). This demonstrates human presence during that period, so an anthropogenic cause for the river channel migration such as direct manipulation of the river course cannot totally be excluded.

Strong fluvial aggradation levels the deepened form of river channels, leading to instability of the river courses since rivers will preferably drain into the deepest geomorphic form (Wells and Dorr, 1987). The channel migration occurred during a regional fluvial aggradation period (period d), and thus we think that this was the most likely cause. During this period, the river obviously re-used a preserved valley form in the eastern part of the alluvial surface. Given the preserved former western river bed, depending on its autogenic sedimentation dynamics, the lower Shulaveris Ghele River can apparently switch between two possible modes during aggradation periods, i.e., choose one of the two inherited river beds (Phillips, 2014).

CONCLUSIONS

Similar to other regional rivers, the lower Shulaveris Ghele River in southeast Georgia aggraded large quantities of mostly fine-grained sediments during the late Pleistocene. These were possibly partly derived from reworked aeolian loess. By comparing the Holocene fluvial dynamics with the neighbouring Algeti River, despite some differences three main aggradation periods indicate enhanced fluvial activity around 6 ka, 3–2, and since about 1 ka. In contrast, prior to about 6 ka, no fluvial aggradation was observed, which possibly indicates weak fluvial activity in a largely stabilized landscape. We assume that fluvial activity was linked to vegetation dynamics that were controlled by regional climatic and/or anthropogenic factors, and for the LIA possibly also to direct climatic forcing. Differences between both rivers could possibly be explained with different tectonic settings, small-scale variations of natural or anthropogenic conditions, or different internal thresholds of the rivers. Whereas our study suggests a completely different fluvial pattern in the southern Caucasus compared with the eastern Mediterranen basin, some similarities appear with eastern Anatolia. Since this conclusion is based on the investigation of just two rivers, further research is needed to better understand the largely independent flooding pattern in the southern Caucasus during the late Quaternary.

Our study suggests that the lower Shulaveris Ghele River did not use its present eastern bed between about 30 and 6 ka. Thus,

the two late Neolithic settlements that are located next to the present eastern river bed were originally not built close to that river. Accordingly, their archaeological record cannot be explained with former river activity, and the lack of direct water access, (yet detected) wells and water reservoirs might suggest water management systems similar to other Neolithic cultures in semi-humid to arid regions of the Near East.

ACKNOWLEDGMENTS

SUPPLEMENTARY MATERIAL

For supplementary material/s referred to in this article, please visit https://doi.org/10.1017/qua.2017.80

REFERENCES

Akhundov, T., 2004. South Caucasus in the Neolithic and early Bronze Age: The question of epochs and periods. In: Sagona, A. (Ed.), *A view from the Highlands. Archaeological studies in honour of Charles Burney. Ancient Near East Studies*, supplement 12, Edition Peeters, pp. 421–436.

Benito, G., Macklin, M.G., Zielhofer, C., Jones, A.F., Machado, M.J., 2015. Holocene flooding and climate change in the Mediterranean. *Catena* 130, 13–33.

Berberyan, M., 1997. Seismic sources of the Transcaucasian historical earthquakes. In: Giardini, D., Balassanian, S. (Eds.), *Historical and prehistorical earthquakes in the Caucasus.* NATO ASI Series 2 Environment 28. Kluwer Academic Publishers, Dordrecht, the Netherlands, pp. 233–311.

Bull, W.B., 1972. Recognition of alluvial-fan deposits in the stratigraphic record. In: Rigby, J.K., Hamblin, W.K. (Eds.), *Recognition of Ancient Sedimentary Environments.* Society of Economic Paleontologists and Mineralogists, Special Publication 16. Society for Sedimentary Research, Tulsa, Oklahoma, pp. 63–83.

Chataigner, C., Badalyan, R., Arimura, M., 2014. The Neolithic of the Caucasus. Oxford Handbooks Online. http://dx.doi.org/10.1093/oxfordhb/9780199935413.013.13.

Collins, P.E.F., Rust, D.J., Bayraktutan, M.S., Turner, S.D., 2005. Fluvial stratigraphy and palaeoenvironments in the Pasinler Basin, eastern Turkey. *Quaternary International* 140–141, 121–134.

Connor, S.E., Kvavadze, E.V., 2008. Modelling late Quaternary changes in plant distribution, vegetation and climate using pollen data from Georgia, Caucasus. *Journal of Biogeography* 36, 529–545.

Connor, S.E., Sagona, A., 2007. Environment and society in the Late Prehistory of Southern Georgia, Caucasus. In: Lyonnet, B. (Ed.), *Les Cultures du Caucase (VIe-IIIe millénaires avant notre ère): leurs relations avec le Proche-Orient.* CNRS, Éditions Recherche sur les Civilisations. Centre National de la Recherche Scientifique, Paris, pp. 21–36.

Connor, S.E., Thomas, I., Kvavadze, E.V., Arabuli, G.J., Avakov, G.S., Sagona, A., 2004. A survey of modern pollen and vegetation along an altitudinal transect in Southern Georgia, Caucasus region. *Review of Palaeobotany and Palynology* 129, 229–250.

Dodonov, A.E., Zhou, L.P., Markovac, A.K., Tchepalygac, A.L., Trubikhina, V.M., Aleksandrovski, A.C., Simakova, A.N., 2006. Middle–Upper Pleistocene bio-climatic and magnetic records of the Northern Black Sea Coastal Area. *Quaternary International* 149, 44–54.

Dreibrodt, S., Lomax, J., Nelle, O., Lubos, C., Fischer, P., Mitsuov, A., Reiss, S., et al., 2010. Are mid-latitude slopes sensitive to climatic oscillations? Implications from an Early Holocene sequence of slope deposits and buried soils from eastern Germany. *Geomorphology* 122, 351–369.

Dreibrodt, S., Lubos, C., Lomax, J., Sipos, G., Schroedter, T., Nelle, O., 2014. Holocene landscape dynamics at the tell Arslantepe, Malatya, Turkey - soil erosion, buried soils and settlement layers, slope and river activity in a middle Euphrates catchment. *The Holocene* 24, 1351–1368.

Dütsch, C., Krbetschek, M.R., 1997. New methods for a better internal 40K dose rate determination. *Radiation Measurements* 27, 377–381.

Faust, D., Zielhofer, C., Baena-Escudero, R., Diaz del Olmo, F., 2004. High-resolution fluvial record of late Holocene geomorphic change in northern Tunisia: climatic or human impact? *Quaternary Science Reviews* 23, 1757–1775.

Fort, J., Pujol, T., Vander Linden, M., 2012. Modelling the Neolithic transition in the Near East and Europe. *American Antiquity* 77, 203–219.

Fuchs, M., 2001. Die OSL-Datierung von Archäosedimenten zur Rekonstruktion anthropogen bedingter Sedimentumlagerung. PhD dissertation, University of Heidelberg, Heidelberg, Germany.

Fuchs, M., Woda, C., Bürkert, A., 2007. Chronostratigraphy of a sediment record from the Hajar mountain range in north Oman: implications for optical dating of insufficiently bleached sediments. *Quaternary Geochronology* 2, 202–207.

Galbraith, R.F., Roberts, R.G., Laslett, G.M., Yoshida, H., Olley, J.M., 1999. Optical dating of single and multiple grains of quartz from Jinmium Rock Shelter, Northern Australia: part I, experimental design and statistical models. *Archaeometry* 41, 339–364.

Gamkrelidze, I.P., 2003. Geological map of Georgia 1:500,000. Georgian State Department of Geology and National Oil Company "SAQNAFTOBI."

Gillmore, G.K., Coningham, R.A.E., Fazeli, H., Young, R.L., Magshoudi, M., Batt, C.M., Rusworth, G., 2009. Irrigation on the Tehran Plain, Iran: Tepe Pardis - the site of a possible Neolithic irrigation feature? *Catena* 78, 285–300.

Gobejishvili, R., 2004. Late Pleistocene (Würmian) glaciation of the Caucasus. In: Ehlers, J., Gibbard, P.L. (Eds.), *Quaternary Glaciations - Extent and Chronology*. Elsevier, Amsterdam, pp. 129–134.

Gogichaishvili, G.P., 2016. Soil erosion in river basins of Georgia. *Eurasian Soil Science* 49, 696–704.

Hamon, C., 2008. From Neolithic to Chalcolithic in the Southern Caucasus: economy and macrolithic implements from

Shulaveri-Shomu sites of Kwemo-Kartli (Georgia). *Paléorient* 34, 85–135.

Hamon, C., Jalabadze, M., Agapishvili, T., Baudouin, E., Koridze, I., Messager, E., 2016. Gadachrili Gora: Architecture and organisation of a Neolithic settlement in the middle Kura Valley (6th millennium BC, Georgia). *Quaternary International* 395, 154–169.

Hansen, S., Mirtskhulava, G., Bastert-Lamprichs, K., 2007. Aruchlo: a Neolithic settlement mound in the Caucasus. *Neo-Lithics* 1/07, 13–19.

Holbrook, J., Schumm, S.A., 1999. Geomorphic and sedimentary response of rivers to tectonic deformation: a brief review and critique of a tool for recognizing subtle epeirogenic deformation in modern and ancient settings. *Tectonophysics* 305, 287–306.

Huntley, D.J., Lamothe, M., 2001. Ubiquity of anomalous fading in K-feldspars and the measurement and correction for it in optical dating. *Canadian Journal of Earth Sciences* 38, 1093–1106.

Javakhishvili, A.I., 1973. *Construction and Architecture of the Settlements of the Southern Caucasus from the 5th to the 3rd Millenium BC*. [In Russian.] Edition Metsnerieba, Tbilisi.

Joannin, S., Ali, A.A., Ollivier, V., Roiron, P., Peyron, O., Chevaux, S., Nahapetyan, S., Tozalakyan, P., Karakhanyan, A., Chataigner, C., 2014. Vegetation, fire and climate history of the Lesser Caucasus: A new Holocene record from Zarishat fen (Armenia). *Journal of Quaternary Science* 29, 70–82.

Juyal, N., Chamyal, L.S., Bhandari, S., Bhushan, R., Singhvi, A.K., 2006. Continental record of the southwest monsoon during the last 130 ka: evidence from the southern margin of the Thar desert, India. *Quaternary Science Reviews* 25, 2632–2650.

Keggenhoff, I., Elizbarashvili, M., Amiri-Farahani, A., King, L., 2014. Trends in daily temperature and precipitation extremes over Georgia, 1971–2010. *Weather and Climate Extremes* 4, 75–85.

Kiguradze, T., 1986. Neolithische Siedlungen von Kvemo Kartli, Georgien. Materialien zur allgemeinen und vergleichenden Archäologie. Edition C.H. Beck, München.

Kiguradze, T., 2000. The Chalcolithic - Early Bronze Age transition in the eastern Caucasus. In: Marro, C., Hauptmann, A. (Eds.), Chronologies des pays du Caucase et de l'Euphrate aux IVe-IIIe millénaires. Actes de Colloque d'Istanbul, 16–19 décembre 1998. *Varia Anatolica* 11, 321–328.

Kvavadze, E., Jalabadze, M., Shakulashvili, N., 2010. Arguments indicating the presence of wine in Neolithic pots from Georgia using the method of palynological and chemical analysis. In: *Proceedings of the 33rd World Congress of Vine and Wine and the 8th General Assembly of the International Organisation of Vine and Wine, 20–25 June 2010, Tbilisi, Georgia*. International Organisation of Vine and Wine, Tbilsi, Georgia, pp. 123–132.

Lang, A., Hönscheid, S., 1999. Age and source of colluvial sediments at Vaihingen–Enz, Germany. *Catena* 38, 89–107.

Leopold, L.B., Wolman, L.G., Miller, J., 1964. *Fluvial Processes in Geomorphology*. W.H. Freeman and Co, San Francisco.

Lordkipanidze, O., 2002. Georgien—Land und Raum. In Gambaschidze, I., Hauptmann, A., Slotta, R., Yalcin, Ü. (Eds.), *Georgien. Schätze aus dem Land des Goldenen Vlies*. Exhibition Catalogue for October 28, 2001–May 19, 2002. The German Mining Museum in Bochum, Germany, and Centre of Archaeological Research of the Georgian Academy of Science, Tbilisi, Georgia, 2001, pp. 2–53.

Lyonnet, B., Guliyev, F., Bouquet, L., Bruley-Chabot, G., Samzun, A., Pecqueur, L., Jovenet, E., et al., 2016. Mentesh Tepe, an early

settlement of the Shomu-Shulaveri Culture in Azerbaijan. *Quaternary International* 395, 170–183.

Mann, M.E., 2002. Little Ice Age. In: Munn, T. (Ed.), *Encyclopedia of Global Environmental Change*, Vol. I. John Wiley and Sons, Chichester, United Kingdom, pp. 504–509.

Maruashvili, L.I., 1971. *Gemorphology of Georgia: The Relief of the Georgian SSR in the Aspects of Layers, Origin, Dynamics and History*. [In Russian.] Edition Metsnerieba, Tbilisi.

Messager, E., Belmecheri, S., Grafenstein, U.V., Nomade, S., Voinchet, P., Ollivier, V., Mgeladze, A., Lordkipanidze, D., Mazuy, A., Moreau, C., 2013. Palaeoenvironmental records of the last 13 ka in Lesser Caucasus: first data from Paravani Lake (Djavakheti, Georgia). *Quaternary Science Reviews* 77, 125–140.

Mithen, S., 2010. The domestication of water: water management in the ancient world and its prehistoric origins in the Jordan Valley. *Philosophical Transactions of the Royal Society A* 368, 5249–5274.

Murray, A.S., Wintle, A.G., 2000. Luminescence dating of quartz using an improved single-aliquot regenerative-dose protocol. *Radiation Measurements* 32, 57–73.

Nebieridze, L., 2010. *The Tsopi Chalcolithic Culture*. SABC Edition, Tbilisi.

Ollivier, V., Fontugne, M., Lyonnet, B., 2015. Geomorphic response and ^{14}C chronology of base-level changes induced by Late Quaternary Caspian Sea mobility (middle Kura Valley, Azerbaijan). *Geomorphology* 230, 109–124.

Ollivier, V., Fontugne, M., Lyonnet, B., Chataigner, C., 2016. Base level changes, river avulsions and Holocene human settlement dynamics in the Caspian Sea area (middle Kura valley, South Caucasus). *Quaternary International* 395, 79–94.

Phillips, D., 2014. Anastamosing channels in the lower Neches River valley, Texas. *Earth Surface Processes and Landforms* 39, 1888–1899.

Preusser, F., 2003. IRSL dating of K-rich feldspars using the SAR-protocol: Comparison with independent age control. *Ancient TL* 21, 17–23.

Reimer, P.J., Bard, E., Bayliss, A., Beck, J.W., Blackwell, P.G., Bronk Ramsey, C., Buck, C.E., et al., 2013. IntCal13 and Marine13 radiocarbon age calibration curves 0–50,000 years cal BP. *Radiocarbon* 55, 1869–1887.

Rittenour, T.M., 2008. Luminescence dating of fluvial deposits: applications to geomorphic, palaeoseismic and archaeological research. *Boreas* 37, 613–635.

Sahu, S., Raju, N.J., Saha, D., 2010. Active tectonics and geomorphology in the Sone-Ganga alluvial tract in mid-Ganga Basin, India. *Quaternary International* 227, 116–126.

Suchodoletz, H., von, Gärtner, A., Hoth, S., Umlauft, J., Sukhishvili, L., Faust, D., 2016. Late Pleistocene river migrations in response to thrust belt advance and sediment-flux steering – the Kura River (southern Caucasus). *Geomorphology* 266, 53–65.

Suchodoletz, H., von, Menz, M., Kühn, P., Sukhishvili, L., Faust, D., 2015. Fluvial sediments of the Algeti River in southeastern Georgia – an archive of Late Quaternary landscape activity and stability in the Transcaucasian region. *Catena* 130, 95–107.

Tokuyasu, K., Tanaka, K., Tsukamoto, S., Murray, A., 2010. The characteristics of OSL signal from quartz grains extracted from modern sediments in Japan. *Geochronometria* 37, 13–19.

Torrent, J., Liu, Q., Bloemendal, J., Barrón, V., 2007. Magnetic enhancement and iron oxides in the upper Luochuan loess–paleosol

sequence, Chinese Loess Plateau. *Soil Science Society of America Journal* 71, 1570–1578.

Vincent, P.J., Lord, T.C., Telfer, M.W., Wilson, P., 2010. Early Holocene loessic colluviation in northwest England: new evidence for the 8.2 ka event in the terrestrial record? *Boreas* 40, 105–115.

Vlaminck, S., Kehl, M., Lauer, T., Shahriari, A., Sharifi, J., Eckmeier, E., Lehndorff, E., Khormali, F., Frechen, M., 2016. Loess-soil sequence at Toshan (Northern Iran): Insights into late Pleistocene climate change. *Quaternary International* 399, 122–135.

Wells, N.A., Dorr, J.A., 1987. Shifting of the Kosi River, northern India. *Geology* 15, 204–207.

Wirth, S., Glur, L., Gilli, A., Anselmetti, F.S., 2013. Holocene flood frequency across the Central Alps - solar forcing and evidence for variations in North Atlantic atmospheric circulation. *Quaternary Science Reviews* 80, 112–128.

Wolf, D., Baumgart, P., Meszner, S., Fülling, A., Haubold, F., Sahakyan, L., Meliksetian, K., Faust, D., 2016. Loess in Armenia – stratigraphic findings and palaeoenvironmental indications. *Proceedings of the Geologists Association* 127, 29–39.

Zielhofer, C., Recio-Espejo, J.M., Nunez-Granados, M.A., Faust, D., 2009. Durations of soil formation and soil development indices in a Holocene Mediterranean floodplain. *Quaternary International* 209, 44–65.